Reducing Actuator Requirements in Continuum Robots through Optimized Cable Routing: Supplementary Information

Jennifer C. Case, Edward L. White, Vytas SunSpiral, Rebecca K. Kramer

May 24, 2017

1 Model Derivation

Start with free end of the model, on the jth segment.
Sum of forces:

$$\sum \mathbf{F} = 0$$
$$\mathbf{F}_{R,j} + \sum_{i=0}^{n-1} {}^{j}\mathbf{R}^{e}{}_{e'}\mathbf{F}_{T_i,j} = 0$$
$$\mathbf{F}_{R,j} = -\sum_{i=0}^{n-1} {}^{j}\mathbf{R}^{e}{}_{e'}\mathbf{F}_{T_i,j}$$
$$\mathbf{F}_{R,j} = \sum_{i=0}^{n-1} T_i \begin{Bmatrix} -\sin\frac{\theta_j}{2} \\ \cos\frac{\theta_j}{2} \end{Bmatrix}$$

where $\mathbf{F}_{R,j}$ is the reaction force of the jth segment, ${}^{j}\mathbf{R}^{e}{}_{e'}$ is the rotation matrix for the jth segment,$\mathbf{F}_{T_i,j}$ is the force vector for the ith cable in the e' frame, θ_j is the angle for the jth segment, and n is the number of cables.
Sum of moments:

$$\sum M = 0$$
$$M_{R,j} + \sum_{i=0}^{n-1} \mathbf{r}_{T_i,j} \times {}^{j}\mathbf{R}^{e}{}_{e'}\mathbf{F}_{T_i,j} = 0$$
$$M_{R,j} = -\sum_{i=0}^{n-1} \mathbf{r}_{T_i,j} \times {}^{j}\mathbf{R}^{e}{}_{e'}\mathbf{F}_{T_i,j}$$
$$M_{R,j} = -\sum_{i=0}^{n-1} T_i d_i \cos\frac{\theta_j}{2}$$

where $M_{R,j}$ is the reaction moment of the jth segment, $\mathbf{r}_{T_i,j}$ is the moment arm from the origin of the e frame to the end of the ith cable.
When we move to the $(j-1)$th segment, we consider the reaction forces from the previous (jth) segment, the cables from the previous (jth) segment, and the cables from the current ($(j-1)$th) segment.

Sum of forces:

$$\sum \mathbf{F} = 0$$

$$\mathbf{F}_{R,j-1} + \sum_{i=0}^{n-1} {}^{j-1}\mathbf{R}^{e}{}_{e'}\mathbf{F}_{T_i,j-1} - \sum_{i=0}^{n-1} {}^{j-1}\mathbf{R}^{e}{}_{e'}{}^{j}\mathbf{R}^{e}{}_{e'}\mathbf{F}_{T_i,j} - {}^{j-1}\mathbf{R}^{e}{}_{e'}\mathbf{F}_{R,j} = 0$$

$$\mathbf{F}_{R,j-1} = -\sum_{i=0}^{n-1} {}^{j-1}\mathbf{R}^{e}{}_{e'}\mathbf{F}_{T_i,j-1}$$

$$\mathbf{F}_{R,j-1} = \sum_{i=0}^{n-1} T_i \begin{Bmatrix} -\sin\frac{\theta_{j-1}}{2} \\ \cos\frac{\theta_{j-1}}{2} \end{Bmatrix}$$

Sum of moments:

$$\sum M = 0$$

$$M_{R,j-1} + \sum_{i=0}^{n-1} \mathbf{r}_{T_i,j-1} \times {}^{j-1}\mathbf{R}^{e}{}_{e'}\mathbf{F}_{T_i,j-1} - M_{R,j} - \mathbf{r}_{j-1} \times {}^{j-1}\mathbf{R}^{e}{}_{e'}\mathbf{F}_{R,j} - \sum_{i=0}^{n-1} \mathbf{r}_{T_i,j-1} \times {}^{j-1}\mathbf{R}^{e}{}_{e'}{}^{j}\mathbf{R}^{e}{}_{e'}\mathbf{F}_{T_i,j} = 0$$

$$M_{R,j-1} = -\sum_{i=0}^{n-1} \mathbf{r}_{T_i,j-1} \times {}^{j-1}\mathbf{R}^{e}{}_{e'}\mathbf{F}_{T_i,j-1} + M_{R,j} + \mathbf{r}_{j-1} \times {}^{j-1}\mathbf{R}^{e}{}_{e'}\mathbf{F}_{R,j} + \sum_{i=0}^{n-1} \mathbf{r}_{T_i,j-1} \times {}^{j-1}\mathbf{R}^{e}{}_{e'}{}^{j}\mathbf{R}^{e}{}_{e'}\mathbf{F}_{T_i,j}$$

Note that:

$$\mathbf{r}_{j-1} = \begin{Bmatrix} \frac{1}{\kappa_{j-1}}\cos\theta_{j-1} - \frac{1}{\kappa_{j-1}} \\ \frac{1}{\kappa_{j-1}}\sin\theta_{j-1} \end{Bmatrix} \qquad \mathbf{r}_{T_i,j-1} = \begin{Bmatrix} \left(\frac{1}{\kappa_{j-1}} + d_i\right)\cos\theta_{j-1} - \frac{1}{\kappa_{j-1}} \\ \left(\frac{1}{\kappa_{j-1}} + d_i\right)\sin\theta_{j-1} \end{Bmatrix}$$

Using this, we find:

$$\sum_{i=0}^{n-1} \mathbf{r}_{T_i,j-1} \times {}^{j-1}\mathbf{R}^{e}{}_{e'}\mathbf{F}_{T_i,j-1} = \sum_{i=0}^{n-1} T_i d_i \cos\frac{\theta_{j-1}}{2}$$

$$\mathbf{r}_{j-1} \times {}^{j-1}\mathbf{R}^{e}{}_{e'}\mathbf{F}_{R,j} = \sum_{i=0}^{n-1} \frac{T_i}{\kappa_{j-1}}\left(\cos\left(\theta_{j-1} + \frac{\theta_j}{2}\right) - \cos\frac{\theta_j}{2}\right)$$

$$\sum_{i=0}^{n-1} \mathbf{r}_{T_i,j-1} \times {}^{j-1}\mathbf{R}^{e}{}_{e'}{}^{j}\mathbf{R}^{e}{}_{e'}\mathbf{F}_{T_i,j} = -\sum_{i=0}^{n-1} \frac{T_i}{\kappa_{j-1}}\left(\cos\left(\theta_{j-1} + \frac{\theta_j}{2}\right) - \cos\frac{\theta_j}{2}\right) + \sum_{i=0}^{n-1} T_i d_i \cos\frac{\theta_j}{2}$$

Thus, we find our moment to be:

$$M_{R,j-1} = -\sum_{i=0}^{n-1} T_i d_i \cos\frac{\theta_{j-1}}{2}$$

Thus, we can see the equations for both force and moment hold regardless of segment.

2 Experimental Validation

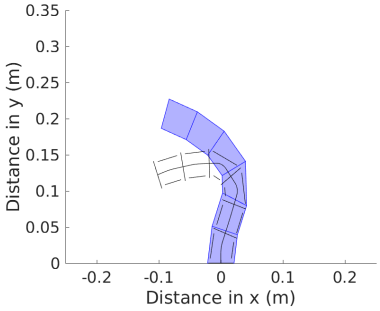

{43,-29.5,32,-20,-19,53.5,-7.5,44}mm
85.4 ± 2.8mm
(a)

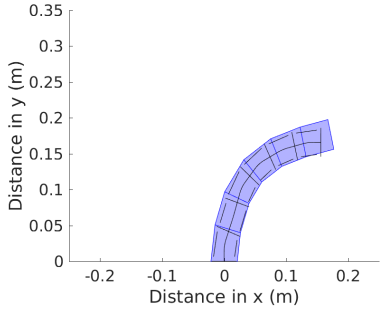

{-18,22.5,-2.5,6.5,34.5,-8.5,17,9.5}mm
20.0 ± 0.9mm
(b)

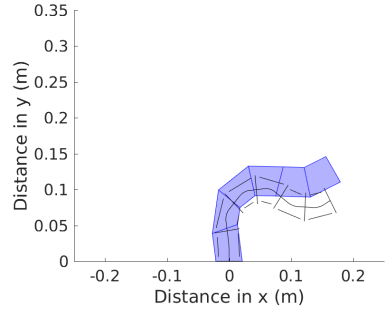

{-5,4,-43.5,71,28.5,18,66.5,-47.5}mm
43.8 ± 5.4mm
(c)

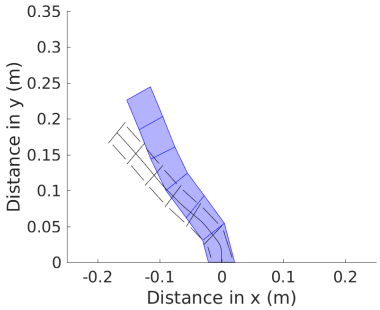

{24,27,21,22,-2.5,-8,-1.5,-2}mm
65.0 ± 2.9mm
(d)

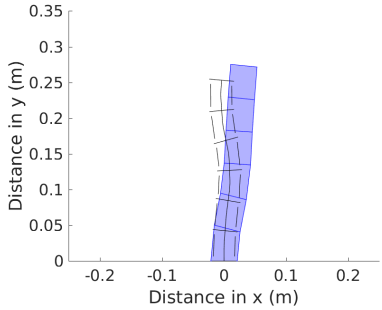

{6.5,5,17.5,-4.5,8.5,12,-0.5,19}mm
41.3 ± 1.0mm
(e)

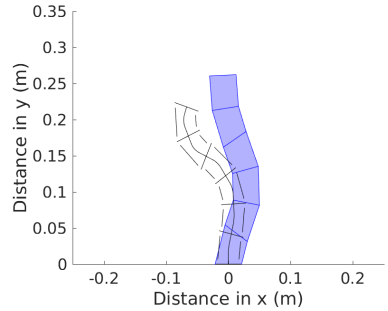

{8.5,19.5,55.5,-37.5,18,5.5,-29.5,63}mm
72.8 ± 1.5mm
(f)

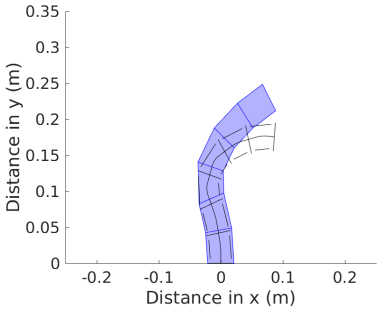

{-15,52,6,22.5,40,-27.5,16.5,0}mm
55.3 ± 0.4mm
(g)

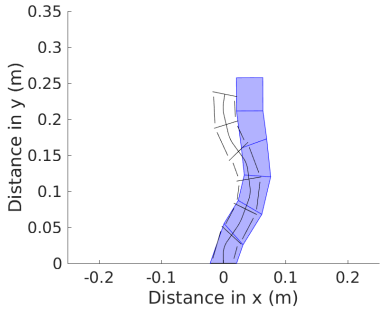

{5.5,-1,35.5,-40,11,19,-17,56}mm
45.9 ± 2.1mm
(h)

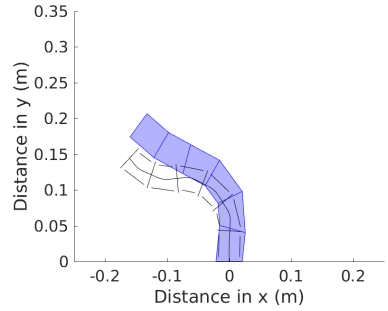

{20.5,17.5,52.5,-36,-3.5,0.5,-33.5,53}mm
48.4 ± 2.1mm
(i)

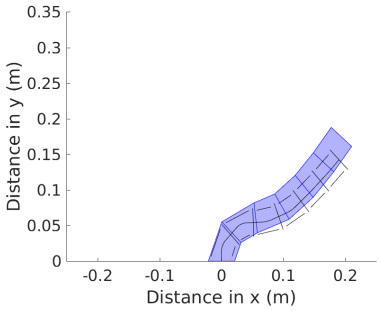

{0,-25.5,-4.5,0.5,23.5,49,27,21}mm
32.6 ± 3.2mm
(j)

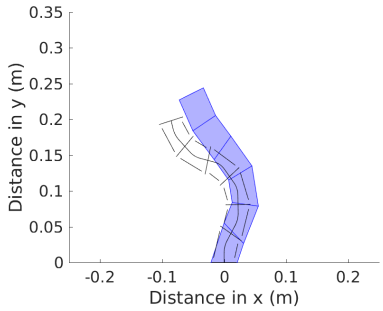

{13,5,48,-49.5,4.5,12.5,-32,66}mm
49.7 ± 5.4mm
(k)

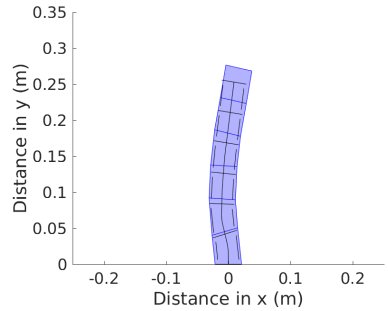

{6,9,4,18.5,10.5,6.5,10,-3.5}mm
21.1 ± 0.5mm
(l)

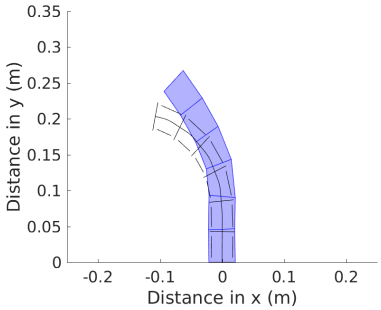

{29.5,-11.5,9,5,-15.5,28,4,10}mm
57.7 ± 7.2mm
(m)

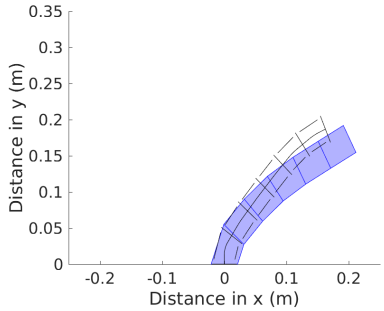

{-10.5,4,1.5,-5,27.5,12,12.5,22.5}mm
41.7 ± 9.4mm
(n)

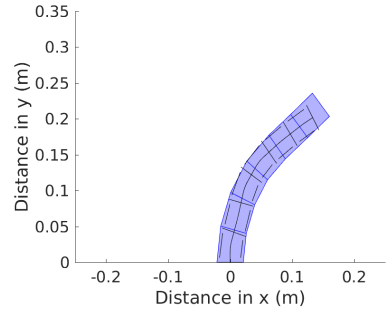

{-10,15.5,-5.5,10.5,25,-2.5,19,4.5}mm
22.3 ± 0.2mm
(o)

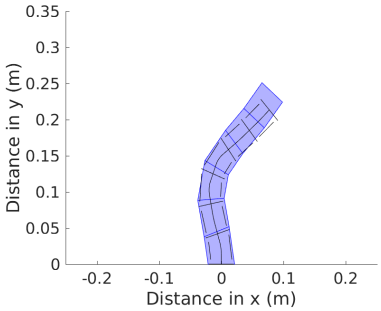

{-6,27.5,-9.5,35,20.5,-11.5,24.5,-18.5}mm
26.2 ± 4.7mm
(p)

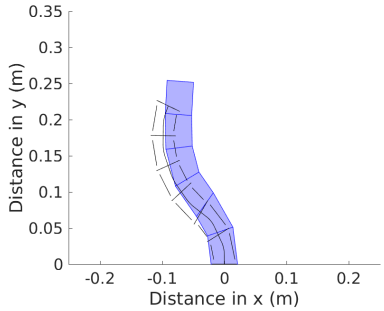

{2.5,48.5,28,6,16,-29.5,-10,11}mm
39.2 ± 2.7mm
(q)

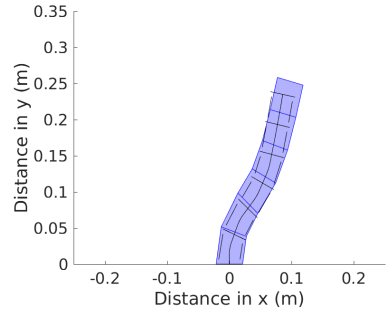

{5,-11.5,3.5,0.5,11,29,12.5,18}mm
22.2 ± 0.7mm
(r)

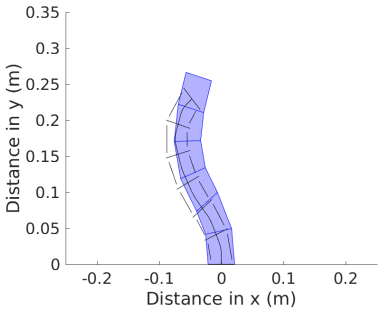

{-5.5,45.5,31,0,22,-28,-14.5,18}mm
34.0 ± 3.5mm
(s)

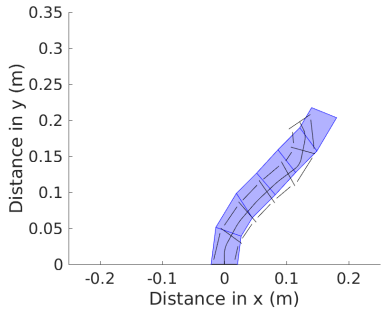

{20.5,-22.5,-28.5,35,4,47,53.5,-11.5}mm
44.1 ± 17.3mm
(t)

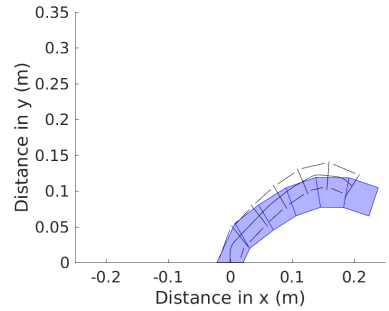

{-26.5,19,10.5,-16.5,46,0.5,10,36}mm
47.7 ± 14.6mm
(u)

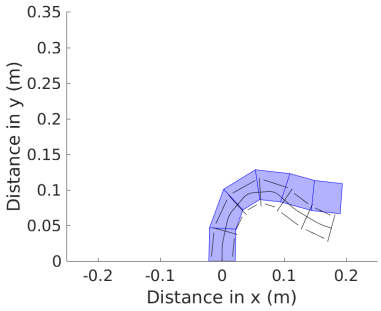

{-21.5,14.5,-33,43.5,39.5,4.5,52,-25.5}mm
44.6 ± 4.4mm
(v)

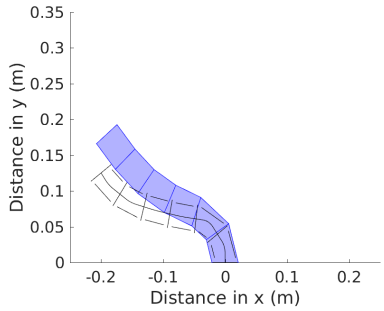

{17,45,41.5,-3.5,-2,-29,-24.5,20}mm
55.2 ± 12.0mm
(w)

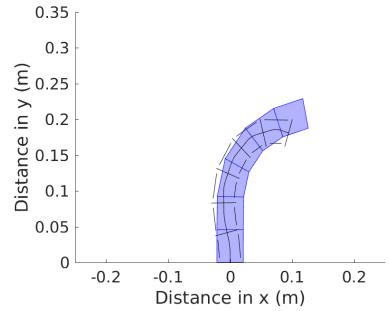

{-19.5,43,16.5,12.5,42.5,-21,5,10}mm
39.1 ± 1.1mm
(x)

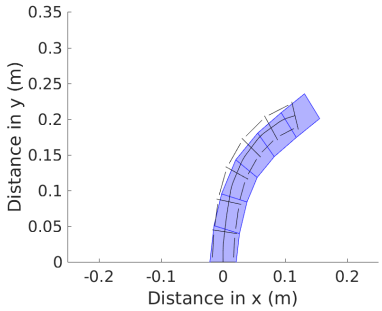

{-14,23.5,6,6.5,29.5,-7.5,10,11}mm
30.9 ± 1.6mm
(y)

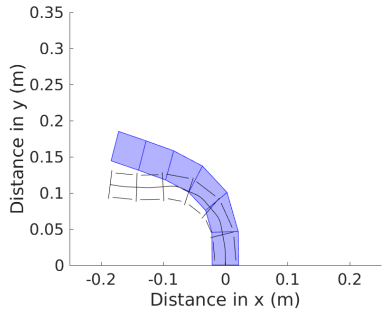

{32.5,11,39,-14.5,-14.5,7,-22.5,32}mm
53.7 ± 5.7mm
(z)

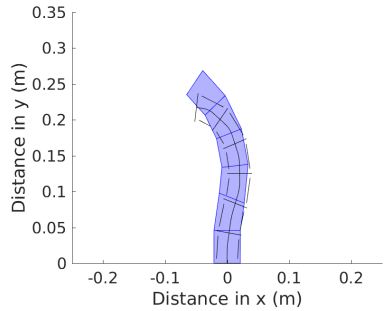

{33.5,-25,-3.5,15,-13.5,44.5,20,1.5}mm
35.1 ± 2.1mm
(A)

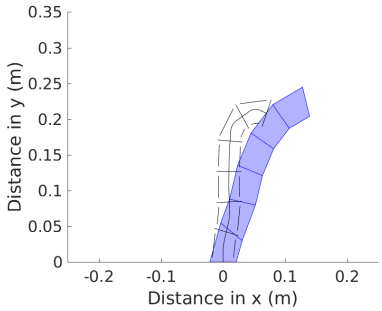

{-20,43.5,40,-27.5,42.5,-22,-18,48}mm
65.6 ± 1.0mm
(B)

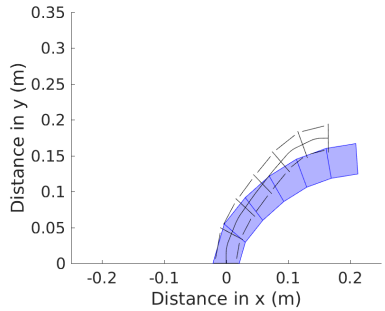

{-19,10.5,5,-7,32.5,3.5,5.5,21}mm
54.4 ± 0.8mm
(C)

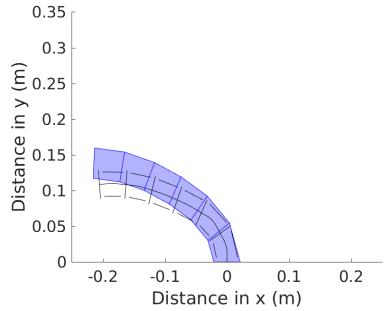

{34.5,15.5,23.5,10,-20,-1,-7.5,4.5}mm
31.4 ± 4.9mm
(D)

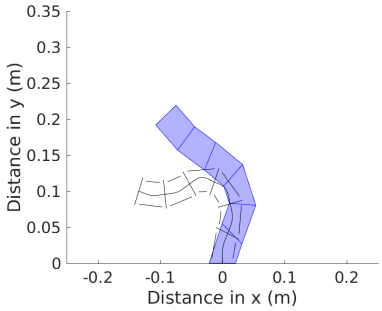

{30.5,0,60.5,-52,-8,22.5,-38.5,74.5}mm
113.9 ± 16.7mm
(E)

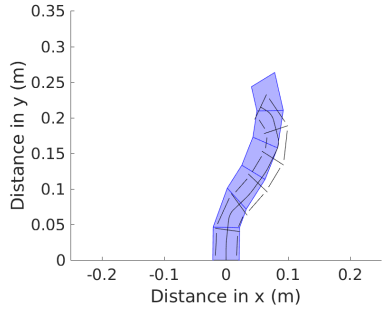

{28.5,-34.5,-23,40.5,-6.5,57.5,45.5,-19}mm
38.9 ± 0.6mm
(F)

Figure S1: Experimental tests for model validation. The recreation of the spine is shaded blue while the model prediction is shown as a black outline. Changes in lengths are listed in the first row and end point error is listed in the second row below the figures.

3 Tension Comparisons between Crossing and Traditional Cable Configurations

Tension comparisons were done using the experimental validation spine positions since this provided a large sample for comparisons. The following table shows the maximum tension for the spine positions using both traditional and crossing cable configurations.

Table S1: Maximum tension for a given spine position. Bolded values are the higher value.

Spine position	Maximum tension (traditional)	Maximum tension (crossing)
Figure 12(b)	**0.813N**	0.714N
Figure 12(c)	0.565N	**0.674N**
Figure 12(d)	**0.826N**	0.636N
Figure S1(a)	**1.195N**	0.680N
Figure S1(b)	0.563N	**0.880N**
Figure S1(c)	**1.775N**	0.721N
Figure S1(d)	**0.716N**	0.648N
Figure S1(e)	0.449N	**0.727N**
Figure S1(f)	**1.675N**	0.606N
Figure S1(g)	**1.146N**	0.734N
Figure S1(h)	**1.305N**	0.737N
Figure S1(i)	**1.288N**	0.597N
Figure S1(j)	**1.480N**	0.791N
Figure S1(k)	**1.615N**	0.750N
Figure S1(l)	0.733N	**0.750N**
Figure S1(m)	0.394N	**0.812N**
Figure S1(n)	0.670N	**0.831N**
Figure S1(o)	0.493N	**0.844N**
Figure S1(p)	**0.811N**	0.671N
Figure S1(q)	**1.030N**	0.511N
Figure S1(r)	0.714N	**0.719N**
Figure S1(s)	**0.742N**	0.586N
Figure S1(t)	**1.109N**	0.822N
Figure S1(u)	**1.149N**	0.702N
Figure S1(v)	**1.244N**	0.588N
Figure S1(w)	**1.213N**	0.717N
Figure S1(x)	**0.715N**	0.607N
Figure S1(y)	0.381N	**0.726N**
Figure S1(z)	**0.693N**	0.586N
Figure S1(A)	0.713N	**0.937N**
Figure S1(B)	**1.337N**	0.770N
Figure S1(C)	0.503N	**0.854N**
Figure S1(D)	0.566N	**0.582N**
Figure S1(E)	**2.002N**	0.723N
Figure S1(F)	**1.290N**	0.838N
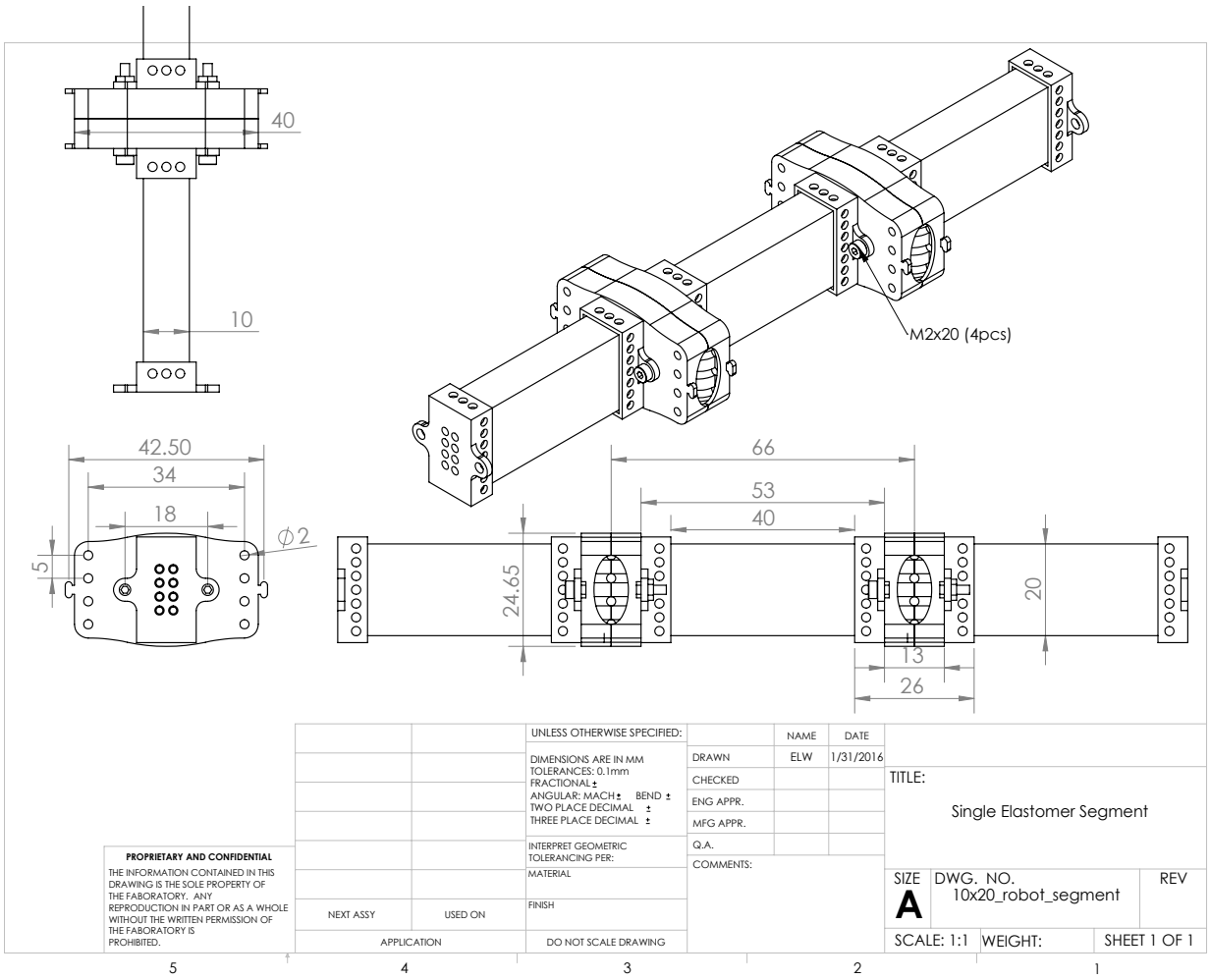
4 Dimensions of Physical System